Tectonic Evolution of the Polydeformed Urf Al-Mahib Belt, South-Eastern Desert, Egypt

Z. Hamimi[a], *****, **M. K. Ghazaly**[b], **E. A. Mohamed**[b], **A. El-Fakharani**[b, c], **and M. Y. Abo-Soliman**[b], *****

[a]*Department of Geology, Faculty of Science, Benha University, Benha, Qalubiya Governorate, P.O.13518 Egypt*
[b]*Department of Geology, Faculty of Science, Aswan University, Aswan, P.O.81528 Egypt*
[c]*Department of Structural Geology and Remote Sensing, Faculty of Earth Sciences, King Abdul Aziz University, P.O. Box 80206, Jeddah, 21589 Saudi Arabia*
*****e-mail: abosoliman.m.y@gmail.com*
Received April 19, 2018; revised July 22, 2019; accepted September 24, 2019

Abstract—The Urf Al-Mahib area, located to the southern part of the Eastern Desert (SED) of Egypt, is covered mainly by juvenile Neoproterozoic crust and Nubian sandstones. Field investigation and structural analyses give evidence that the area of Urf Al-Mahib developed through four successive phases of deformation (D_1, D_2, D_3 and D_4). D_1 was an attenuated phase represented by tight to isoclinal folds (F_1), tightly appressed fold closures and sheared-out hinges, and axial plane foliation (S_1), as well as mineral and stretching lineations (L_1). Structural fabrics formed during the D_2 phase embrace minor- and map-scale prominent F_2 overturned folds with NW (to NNW)-dipping long upper limbs and short lower overturned limbs and axial planes striking NE (to ENE)−SW (to WSW) and dipping to the NW at moderate angles. F_2 folds are geometrically- and kinematically-related to thrust propagation, and often have SE (to SSE) vergence. Thrust faults, that striking NE (to ENE)−SW (to WSW) and dipping NW to NNW, are also common in this stage. D_3 structures contain pervasive vertical to inclined mesoscopic open to very open folds (F_3), whose axes plunge NW (to NNW) and SE (to SSE) at moderate to steep angles. The latest D_4 deformation phase is represented by abundant small- and large-scales WNW−ESE trending dextral semi-ductile-semi-brittle-shear zones.

Keywords: Urf Al-Mahib, South Eastern Desert (SED), Juvenile Neoproterozoic crust, tectonic evolution, Wadi Kharit Shear Zone, transpression, thrust-related folds

DOI: 10.1134/S0016852119060049

INTRODUCTION

The Arabian-Nubian Shield (ANS) comprises the Arabian shield and the Nubian shield which constitute the northern part of the East African Orogen (EAO). This orogen extends for about 6000 km from South India passing through the Arabian Peninsula and eastern Africa in the north to the eastern margin of Kenya and Tanzania, Mozambique, Madagascar, and Antarctica in the south. The Precambrian rocks of the ANS had been evolved during the Neoproterozoic Pan-African Orogeny at ca. 950−550 Ma [7, 11]. The NE Africa was formed as a result of amalgamation of island arcs, which resulted in the formation of nappes that comprise ophiolites, arc volcanics and sedimentary rocks [2, 3, 7, 10, 11] or was formed as accretion of E and W Gondwana [6, 12]. Terranes composed of Neoproterozoic juvenile crusts are characterized by sutures along with linear dismembered ophiolites and mélanges [3, 13]. The Eastern Desert of Egypt occupies the northwestern part of the ANS and the Eastern Desert rocks comprise a lower infrastructural unit and an upper suprastructural unit [1, 3]. Structural study of deformed rocks may have several objectives, one of the principal aims is the establishment of the structural progression [5].

GEOLOGICAL SETTING

The ANS is one of the largest fragments of juvenile Neoproterozoic crust which consists mainly of terranes of intra-oceanic crust and continental crust amalgamated through sutures and/or shear zones. The Urf Al-Mahib area is distinguished by four distinct lithological groups outcropping in the area that have been identified and are arranged tectonostratigraphically (Fig. 1) beginning with the oldest as follows; metasediments, metagabbro-diorite complex, syn-to late-tectonic granitoids, Post-tectonic granites, Post-granite dykes, and Phanerozoic sediments represented essentially by the Nubian sandstone.

Metasediments

Metasediments are widely distributed and cover about 45% of the total study area. They occupy the area around the two flanks of Wadi Kharit valley (or
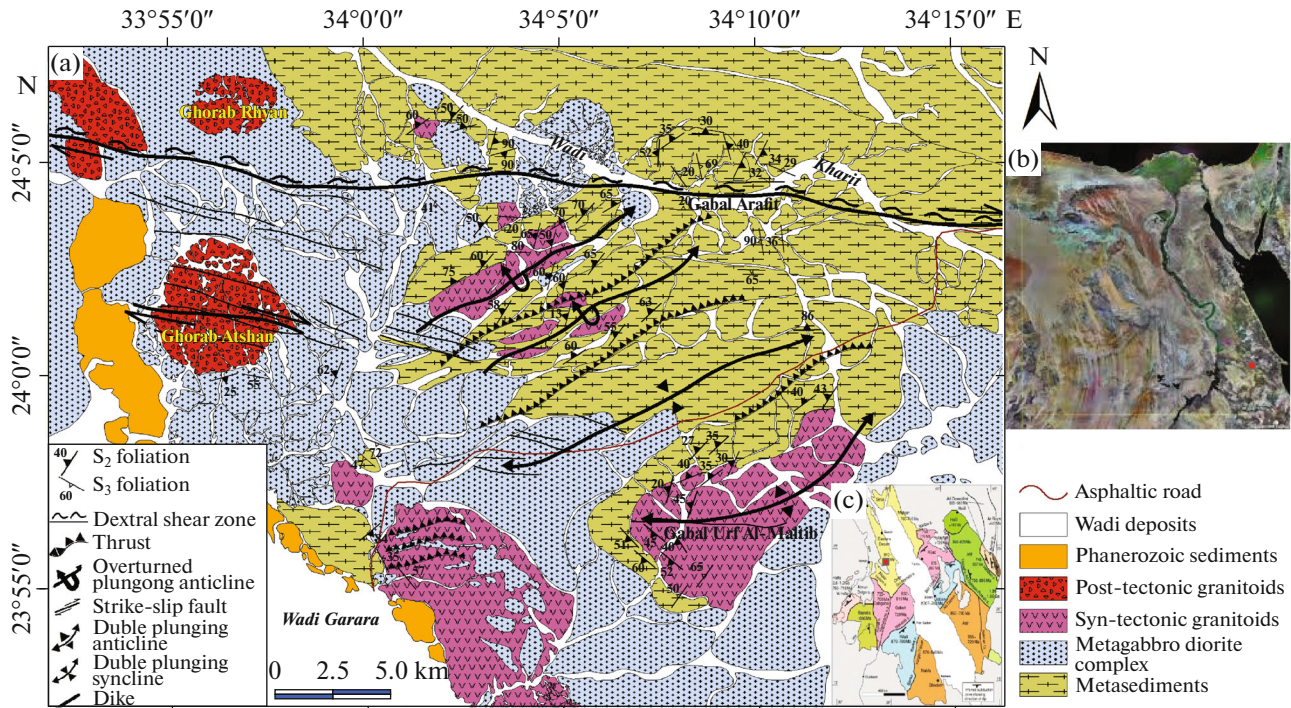
Fig. 1. (a) Geological map of Urf Al-Mahib study area. (b) SPOT image of Egypt showing location of the study area. (c) Terrane map of the ANS after [6, 8] showing location of the study area.

ravine) and extend north- and eastwards beyond the limits of the studied area. Small mappable outcrops occur far to the south along the northern bank of Wadi Garara along the contact of the Nubian Sandstone (Fig. 2a).

The metasediments make up the oldest rock unit in the area under consideration and they form an elongated belt of moderate to low-lying hills represented by homoclinal ridges trending mainly in an E−W direction and dissected by large number of major faults. These ridges are thrown over a number of ENE−WSW double plunging anticlines. A considerable number of these anticlines is overturned, where the overturned limbs dip toward the NW parallel to the major thrust faults in the northern part of the mapped area. The limbs of the Urf Al-Mahib double plunging anticline is one of the most conspicuous landmark in the studied area. The high relief of these metasediments ascribe to a number of long and thick dikes that occur parallel to the main structural pattern of the area and imparting these metasediments (Fig. 1). They are made up of low grade regionally metamorphosed rocks and comprise spotted metasiltstones, metagreywakes and variable schists of volcanosedimentary affinity. These rocks are fine-grained, range in color from dark grey, grayish green, yellowish green to yellowish brown. They are highly foliated, with their foliation planes striking mostly ENE−WSW to NW-SE and dipping 20°−80° NNW to NE respectively (Fig. 2b).

The general foliation trend locally runs ENE−WSW parallel to the trend of shear zones developed along Wadi Kharit. Primary banding was recorded in few places along the eastern end of Wadi Kharit, and it is nearly parallel to the main schistosity. Relict ribble marks and primary lamination were recorded in meta-siltstones forming a primary depositional structure in these rocks [9, 14], indicating a very low grade of metamorphism of these rocks (Fig. 2c). The metasediments are fractured parallel to foliation planes (Fig. 2d) and they are cut by numerous quartz veins, some of which run parallel to foliation planes and exhibit a later brecciation as the host deformed metasediments (Fig. 2e). These quartz veins were boudinated (Fig. 2f) and some of these quartz veins cut the foliation planes (Fig. 2g). Metasediments are reworked into a pencil structure, which may be produced by the intersection of a bedding parallel fabric and a tectonic cleavage as a result of strike-slip faults that cut them perpendicular to a northern shear zone (Fig. 2h). South of Gabal Arafit (Gabal meaning Mountain in Arabic language), quartzo-feldspathic schists become intensively garnetiferous and the regular shape of many garnet crystals suggests that the garnet is post-deformational (Fig. 2i).
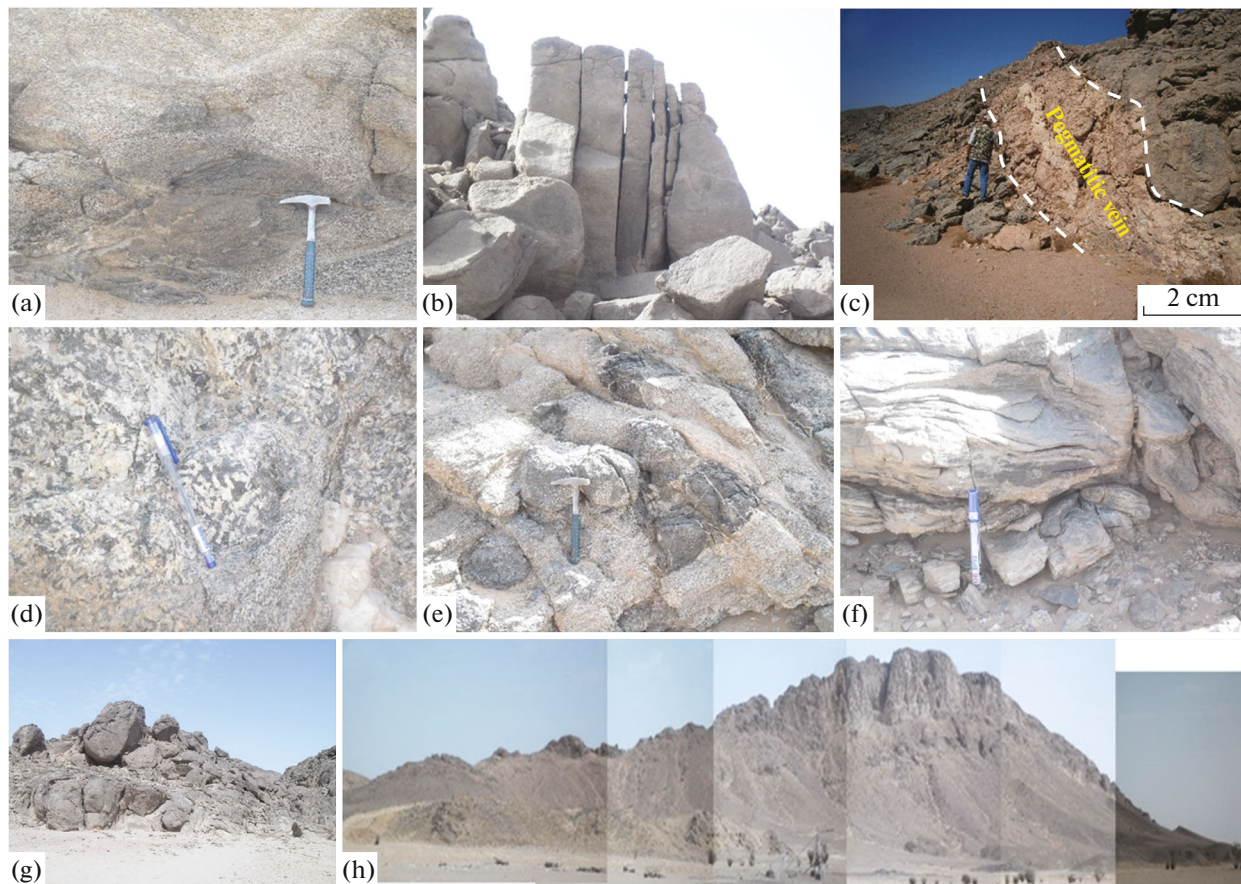
Metagabbro Diorite Complex

The metagabbro-diorite complex occupies an elongated belt stretched in a NW−SE direction,
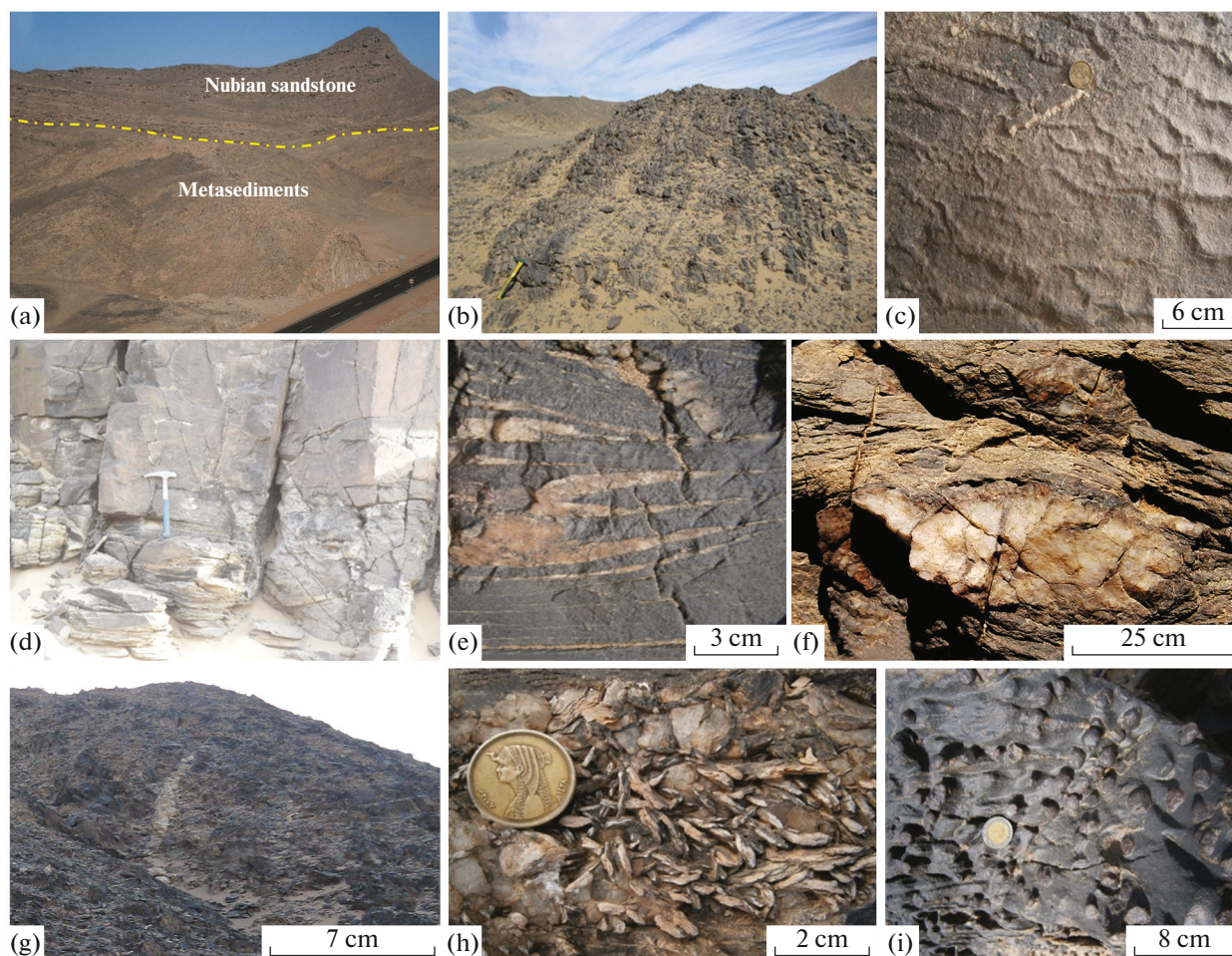
Fig. 2. Field photographs of some features encountered in metasediments. (a) The unconformable relation between Nubian sand stone and the underlying schist along the asphaltic road crossing the northern bank of Wadi Garara. Looking NW. (b) Steeply inclined foliation of dark and light colored schists alternated with each other. (c) Close up view showing relict ribble marks as primary structure inherited from the original sediments. (d) The cleavages planes of metasediments are cut by vertical joints along the two sides of Wadi Kharit. Looking N. (e) Close up view showing quartz vein exhibiting later brecciation traversed highly deformed schist. (f) Close up view showing boudinaged quartz vein within the schists showing right-lateral deformation. (g) Boudinaged quartz vein cutting a cross metasediments foliation. (h) Close up view showing schist separated into pencil structure along one of the strike-slip faults cutting perpendicular to the northern shear zone. (i) Close up view showing garnet crystals in schist, where garnet porphyroclasts stand in relief relative to the fine-grained groundmass. The crystal form of the garnets indicates that they grew largely after deformation.

bounded from the north by the metasediments and intruded in its north-western part by the granite plutons of Ghorab Atshan and Ghorab Rayan whereas it's southern continuation is intruded by two large outcrops of syn- to late-tectonic granites (Fig. 1). The metagabbro-diorite complex composed mainly of metagabbros, quartz diorites and amphibolites. It forms low-to moderate relief, rugged hills or irregular masses separated from each other by minor sandy valleys. These rocks are medium to coarse grained, green or grey to light grey in color and largely massive but occasionally foliated along the peripheral parts, the foliation plane predominately striking N−S. Ex-foliation is commonly obvious, the syn-to late-tectonic granites captured a lot of irregular to spindle like xeno-

liths of metagabbros attains 40 cm−1 m long (Fig. 3a). The spindle shape xenoliths are usually running concordant with the foliation planes of the host granite. A set of NE−SW systematic vertical joints cut across the quartz-diorite (Fig. 3b), and occasionally the joint planes are filled with pegmatite or aplite veins (Fig. 3c). The screens of aplite may cover the roof of the quartz-diorite mass imparting to it smooth surface. The contacts with the granitic rocks of Ghorab Atshan and Ghorab Rayan are knife sharp without any sign of interaction or xenolith content, whereas the contacts with the syn-to late-tectonic granites are rather gradational with a narrow hybrid zone in between. The hybrid zone is marked by lighter colored diorite-looking rocks towards the granite border (Fig. 3d). Fresh,

Fig. 3. Field photographs of some features encountered in Metagabbro diorite complex and Granitic rocks. (a) Close up view showing spindle-shape swarm of metagabbroic xenoliths in quartz- diorite. (b) Field photo showing a vertical joint set cut across the quartz-diorite. (c) Field photo showing a nearly vertical or steeply inclined pegmatitic vein (20−30 cm thick) chilled along periphery with quartz, cutting across quartz-diorite. (d) Close up view showing narrow zone of hybrid diorite produced from the interaction of quartz diorite with gneissose granite. (f) Close up view showing recumbent fold in amphibolites. (g) Field photo showing the outer periphery of Ghorab Atshan. (h) Panoramic view of Gabal Arafit dike.

dark green gabbroic relics are found within the dioritic rocks. Such relics are commonly surrounded by a thin matrix of leucocratic dioritic material, which merge gradually into the host diorite rocks (Fig. 3e). These hybrid rocks may become of pegmatite nature approaching appinites. A series of recumbent folds developed in the amphibolites that associated with metagabbros and most of their axes plunge due to NW (Fig. 3f).

GRANITIC ROCKS

Syn-Tectonic Granitoids

The syn- to late-tectonic granitoids form three main irregular outcrops around the center of the geologic map. This rock unit displays most of the essential features of the granitoid rocks that are syn-tectonically emplaced along shear zones and major thrusting planes in order to accommodate NNW to SSE-transportation, propagation and crustal relaxation of the Pan-African belt [3, 4]. Although these granites send off-shoots into all-encompassing lithologic units revealing its intrusive nature opposed to these units, they show intensively cataclased, foliated or even mylonitized outer margins and less deformed inner core. Taken Urf Al-Mahib granodiorites as a model, and other than cataclases and mylonitization, the rock exhibits well developed open folds and kink bands principally in the outer margins (Fig. 1). Based on these curiosity field relations and observations, it can be stated with reasonable confidence that pluton-emplacement is affiliated to the same deformation phase responsible for the initiation and propagation of thrusting.

In the present work, the Syn-to late-tectonic granitoids are represented by granodiorites and tonalities. Two of the most spectacular structural features of these granites are their distribution at the core of double plunging anticline of Urf Al-Mahib (Fig. 1) and their occurrence as a result of thrust propagation in the center of the mapped area. They have low to moderate relief, circular and elliptical shaped masses, scattered hills, grey, medium to coarse grained, highly weathered, deformed, jointed and exfoliated (Fig. 1).

Post-Tectonic Granitoids

The Post tectonic granites form moderate to high relief country, and are expressed mainly by the alkaline two feldspars, Ghorab Atshan and Ghorab Rayan granite plutons as remarkable landmarks. They have rugged surfaces, high relief and semicircular in shape. Ghorab Atshan area is about 28 km^2, elongated in E−W direction and sending offshoots intruding the surrounding older rocks. Ghorab Atshan is surrounded by moderately elevated (Fig. 3g), coarse grained, highly weathered, exfoliated metagabbroic rocks. Ghorab Rayan area is about 12 km^2, elongated in N−S direction and hasn't any contact relations with the surround rocks being separated from them by a circular wide sandy planes.

Post-Granite Dykes

The basement rocks of the study area are cut by several basic, intermediate and acidic dikes as well as pegmatites and quartz veins. The basic and acidic dikes are predominant whereas intermediate dikes are relatively subordinate. All the dikes are resistant to weathering giving rise to pronounced ridges that cut across the country rocks. Branching of the dikes is recorded along conjugated fractures. These dikes exhibit a marked variation in color, texture, grain size and mineral composition. Some dikes show distinctive swelling and pinching in thickness; although the majority attains a uniform thickness. They are mostly vertical, vary in width from 0.7 to 5 m and extend to long distances (up to four kilometers in length).Sometimes, they form swarms running parallel to each other as in the case of Gabal Arafit dikes (Fig. 3h).

Nubian Sandstone

The basement rocks of the study area are covered by Phanerozoic rocks to the western boarder of the mapped area through sporadic locations (Fig. 1). These Phanerozoic rocks represented by Nubian Sandstone that overlaid the basement rocks through basal conglomerate (Fig. 1). These sandstones are well sorted, medium to coarse grained, range in thickness from a few meters to tens of meters. Some primary structures are still preserved in these rocks.

STRUCTURAL FRAME WORK

Generally, structures in Urf Al-Mahib area can be classified into two main groups; relics of primary structures and secondary structures that comprise planar and linear structures.

Relics of Primary Structures

The primary structures are common in Nubian Sandstone such as; ripple marks, cross bedding, bedding and graded bedding. Also, relics of some primary structures were inherited in metasediments. Relics of ribble marks and primary lamination and bedding were recorded in meta-siltstones forming primary depositional structure in these rocks (Fig. 2c).

Secondary Structures

Secondary structures of the basement rocks include structures that formed by ductile deformation and structures related to the brittle deformation. Ductile deformation structures are represented by planar, foliation planes, and linear structural elements. The latter comprise; fold hinges, mineral lineation, stretching lineation, crenulation lineation, intersection lineation and boudinage structure. The planar and linear structural elements are used to build a model of the macroscopic structures of the area around Urf Al-Mahib. Conventional geometrical analysis was carried out on the poles of planar structures and plunge of lineations of mesoscopic structural elements on lower hemisphere equal area stereonet (Schmidt net). Collected measurements are plotted and contoured using "Spheristat 3.2.1" Software Program [15].

Geometrical Analysis of Ductile Structures

Total of 275 orientation measurements of S-surfaces (foliations) were collected. $S_1//S_0$ foliation is to some extent difficult to be recognized in the field, and the $S_2//S_1$ strike NE (to ENE)−SW (to WSW) and dipping 20°−80° towards NW (to NNW). S_3 strike NW (to NNW)−SE (to SSE) and dipping 60°−88° towards NE (ENE) and/or SW (WSW). Fold hinges indicate that the area around Urf Al-Mahib major fold exhibits F_2 and F_3 folding; both F_1 and F_4 folding are not recognized. F_2 folding plunges NE (to ENE) and/or SW (to WSW) at moderate angles, F_3 Folding is less common and plunges NW (to NNW) and SE (to SSE) at moderate to steep angles. The selected area is subdivided into four structurally homogenous domains (Fig. 4) based on the general structure of the selected area.

(1) Domain I. In this domain structural elements; S_2 foliation, L_2 lineation, F_2 minor fold axes of the D_2 deformation phase are sporadic and difficult to be measured. L_2 lineation and F_2 fold axes form a remarkable concentration, plunging 20° on a bearing N55° E (Fig. 5a, b). The poles to S_2 foliation spread over a great circle pattern, striking N67° W and dipping 36° SW (Fig. 5c). The pole of the great circle defines the $β_2$ (plunging 44° on a bearing N23° E) (Fig. 5d), which nearly coincides with the attitudes of the scarce readings of F_2 and L_2; $β_2 ≈ F_2$ and L_2. The third deformation phase lineation, L_3, and axes of F_3 minor folds, form a noteworthy concentration, plunging 67° on a bearing N27° W (Figs. 5e, 5f). The poles to S_3 foliation exhibit a great circle, striking N 66° E and dipping 8° SSE (Fig. 5g). The pole of the S_3 great
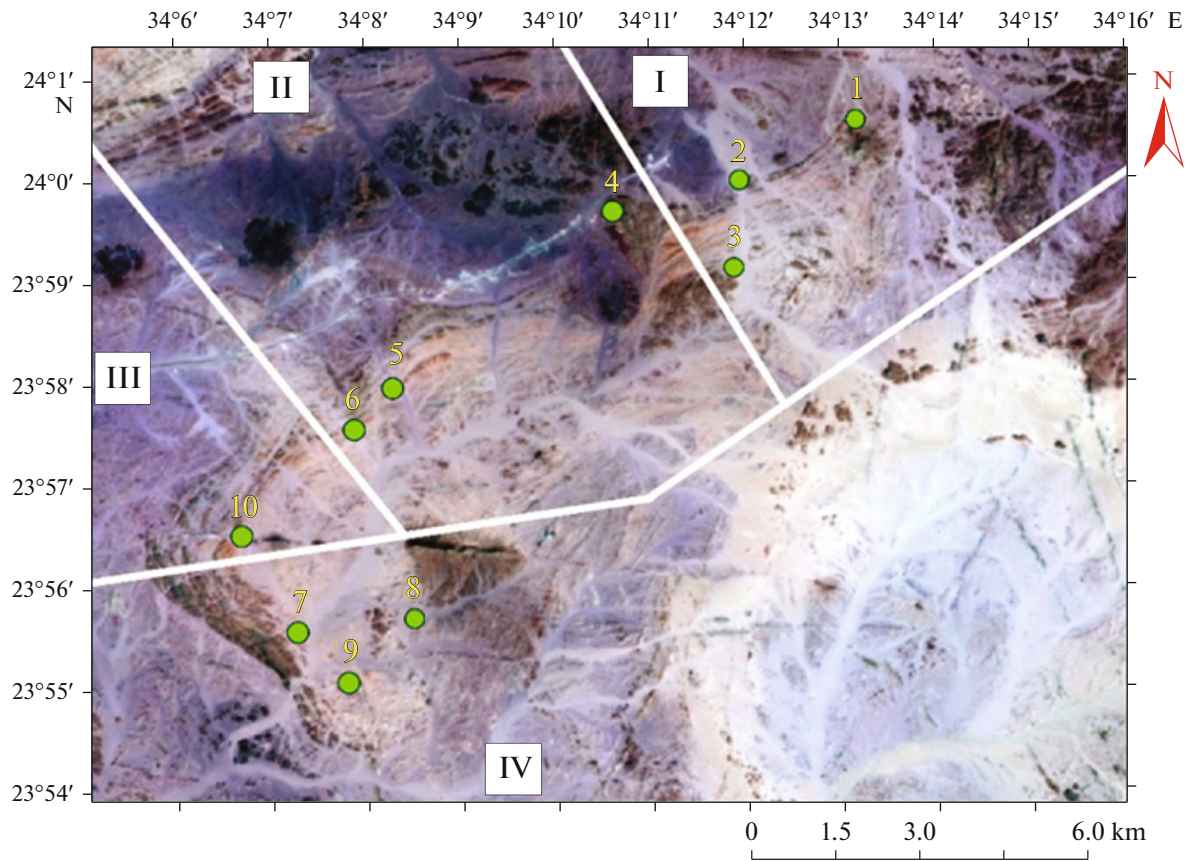
Fig. 4. A Landsat image showing structural domains and observation points (stations) in the sector around Urf Al-Mahib major structure.

circle β_3 (plunging 82° on a bearing N24° W) to some extent coincides with the mean of the maximum concentration of F_3 and L_3; $\beta_3 \approx F_3$ and L_3 (Fig. 5h).

(2) Domain II is the most prominent one that has various and lots of structural data. Structural data of the D_2 deformation phase are represented by L_2 lineation, F_2 minor fold axes and S_2 foliation. Readings of L_2 lineation and F_2 minor fold axes form a remarkable concentration, plunging 40° on a bearing N34° E (Figs. 6a, 6b). The poles to S_2 foliation spread over a great circle pattern, striking N79° W and dipping 57° SW (Fig. 6c). The pole of the great circle defines the β_2 (plunging 33° on a bearing N11° E) which is roughly fitted with the attitudes of the scarce readings of F_2 and L_2; $\beta_2 \approx F_2$ and L_2 (Fig. 6d). The third deformation phase lineation, L_3, and axes of F_3 minor folds, form a remarkable concentration, plunging 56° on a bearing N45° W (Figs. 6e, 6f). The poles to S_3 foliation exhibit a great circle, striking N43° E and dipping 64° SE (Fig. 6g). The pole of the S_3 great circle (β_3; plunging 26° on a bearing N47° W) is slightly deviated from the mean of the maximum concentration of F_3 and L_3 (Fig. 6h).

(3) Domain III. This domain has scarce measurements and readings of L_2 lineation and F_2 minor folds feeble concentration, plunging 40° on a bearing N34° W (Figs. 7a, 7b). The poles to S_2 foliation spread over a great circle pattern, striking N64° E and dipping 59° SE. The pole of the great circle defines the β_2 (plunging 31° on a bearing N26° W) which nearly coincides with the attitudes of the F_2 and L_2; $\beta_2 \approx F_2$ and L_2 (Figs. 7c, 7d). Measurements of the third deformation phase lineation (L_3) and F_3 minor fold axes, as well as S_3 are insufficient to be stereographically plotted in this domain.

(4) Domain IV. Structural data of Domain IV are elements of the D_2 deformation phase are manifested by L_2 lineation, F_2 fold axes and S_2 foliation. L_2 and F_2 form a noticeable concentration, plunging 47° on a bearing N61° E (Figs. 8a, 8b). The poles to S_2 foliation spread over a great circle pattern, striking S50° E and dipping 46° SW (Fig. 8c). The pole of the great circle defines the β_2 (plunging 44° due to N40° E) which nearly coincides with the attitudes of the scarce readings of F_2 and L_2; $\beta_2 \approx F_2$ and L_2 (Fig. 8d). The poles to S_3 foliation exhibit a great circle, striking N36° W and dipping 75° NE (Fig. 8e). The pole of the S_3 great circle (β_3; plunging 15° on a bearing S36° W) (Fig. 8f).

RESULTS AND DISCUSSION

D_1 Deformation Phase

The original banding or layering (S_0) is not easily detected either at the hand specimen-scale or at the outcrop-scale, because it is mostly obliterated due to the effect of the subsequent deformations. S_0, when recorded, is defined by the variations of colors, composition, grain size and layer thickness that composes the predominantly rhythmic units that exist in the area. Structures designated as D_1 include tight to very tight isoclinal folds (F_1), tightly appressed fold closures and sheared-out hinges, and associated axial plane foliation (S_1), as well as mineral and stretching lineations (L_1). D_1 fabrics are quite weak and commonly show different styles in different deformed lithologies. They comprise small- and large-scale isoclinal and intrafolial folds, here designated as F_1, found in the metasediments. In some places of the mapped area, F_1 folds become overturned and are locally southward verging. In other places, only tightly appressed folds and sheared out hinges are observed, and the attitudes of F_1 fold axes show variable orientations due to the effect of latter deformations. Because F_1 is reworked by subsequent D_2, D_3 and D_4 deformations, it is hard to restore F_1 to its original orientation. Parallel to the F_1 fold axial plane is $S_1//S_0$ that is usually a transposing and intrafolial foliations; $S_1//S_0$ surface is isoclinally folded and appears as fold hooks within other $S_1//S_0$ foliation reflecting a progressive transposition. $S_1//S_0$ foliations mostly show a preferred orientation. On $S_1//S_0$ foliation planes, L_1 lineations are defined by preferred orientation of synkinematic minerals. Most of L_1 mineral and stretching lineations show variable orientations most probably due to the effect of the subsequent deformation phases. Of interest to denote that primary sedimentary structures and some magmatic fabrics were usually flattened and rotated parallel to the S_1 foliation that is locally axial planar to coeval F_1 isoclinal folds.
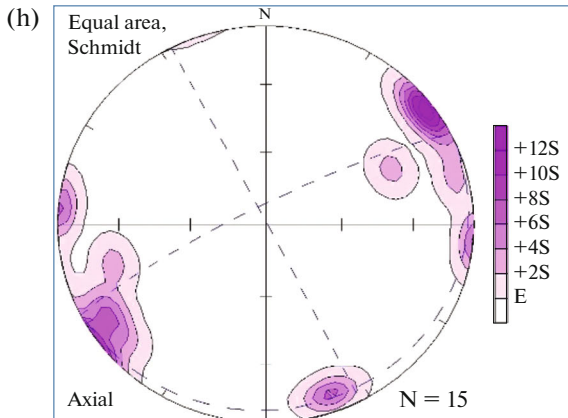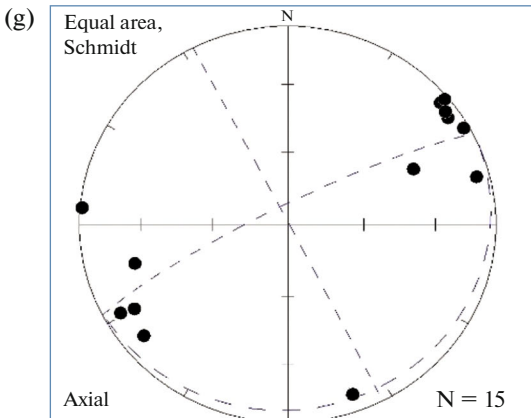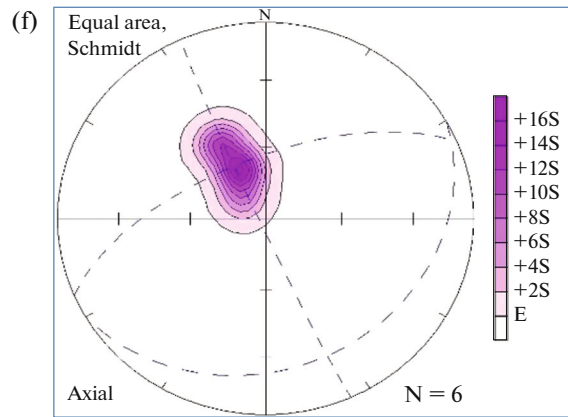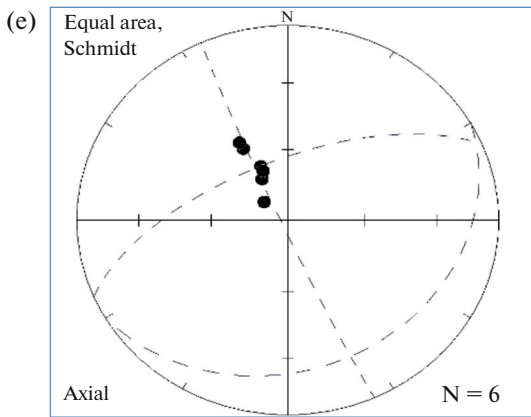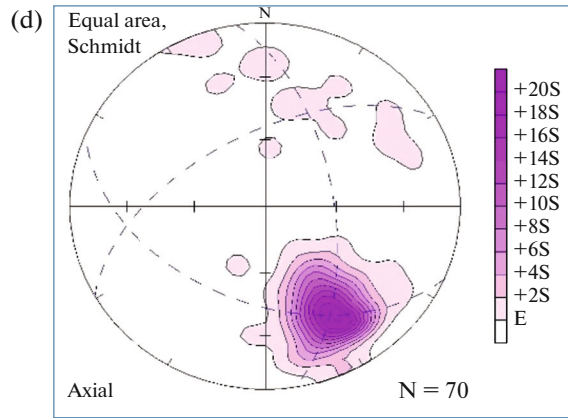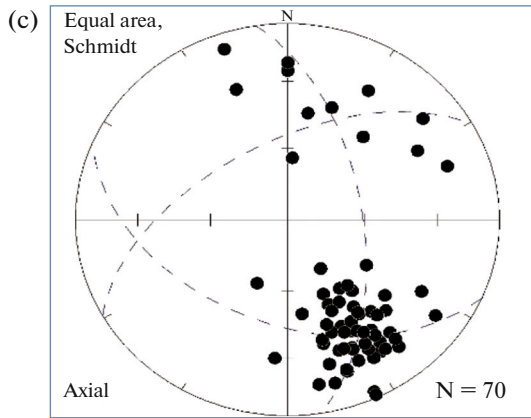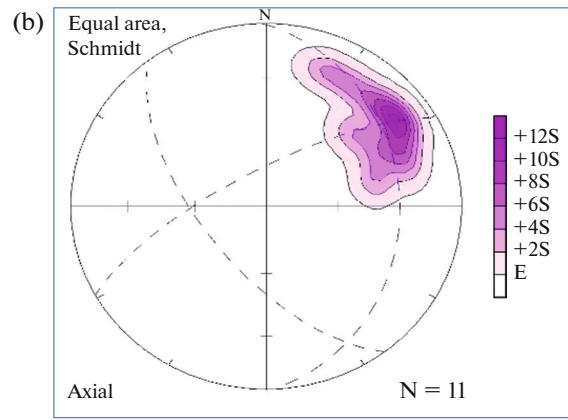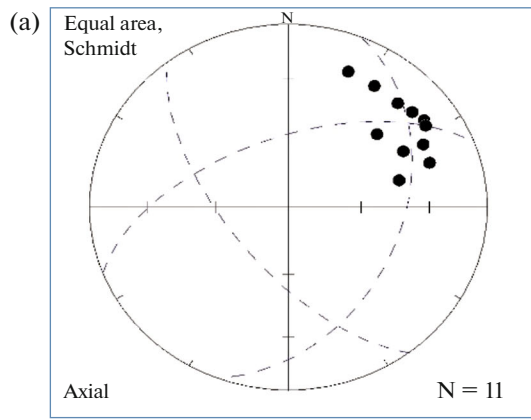
D_2 Deformation Phase

The D_2 deformation phase was quite intense in the exposed rocks of the study area and was probably caused by the continuous shortening in NW-SE direction that began in D_1 during progressive deformation. D_2 is defined by a penetrative foliation S_2 ($//S_1$) filled with products from crystallization of mineral constituents oriented in relation to the S_2 plane. $S_2//S_1$ defines the main plane of rock foliation and has an average attitude striking NE (to ENE)–SW (to WSW) and dipping NW (to NNW) at moderate to steep angles. At Urf Al-Mahib major fold the $S_2//S_1$ dip NW (to NNW) and SE (to SSE). Structural fabrics formed during the D_2 phase embrace minor- and map-scale prominent F_2 overturned folds with NW (to NNW)-dipping long upper limbs and short lower overturned limbs and axial planes striking NE (to ENE)–SW (to WSW) and dipping NW. F_2 folds are geometrically- and kinematically-related to thrust propagation, and often have SE (to SSE) vergence. On map scale, thrusts show the same attitude of the F_2 axial traces and on outcrop-scale thrusting demonstrates flat-ramp-flat geometry. On the limbs of the F_2 thrust-related overturned folds, well developed L_2 elongation and mineral lineations, as well as boudinage structure, are observed. L_2 lineations are coaxial to F_2 folding axes; plunging NE (to ENE) and/or SW (to WSW) at moderate angles. ENE–WSW shortening phase ENE–WSW shortening phase.
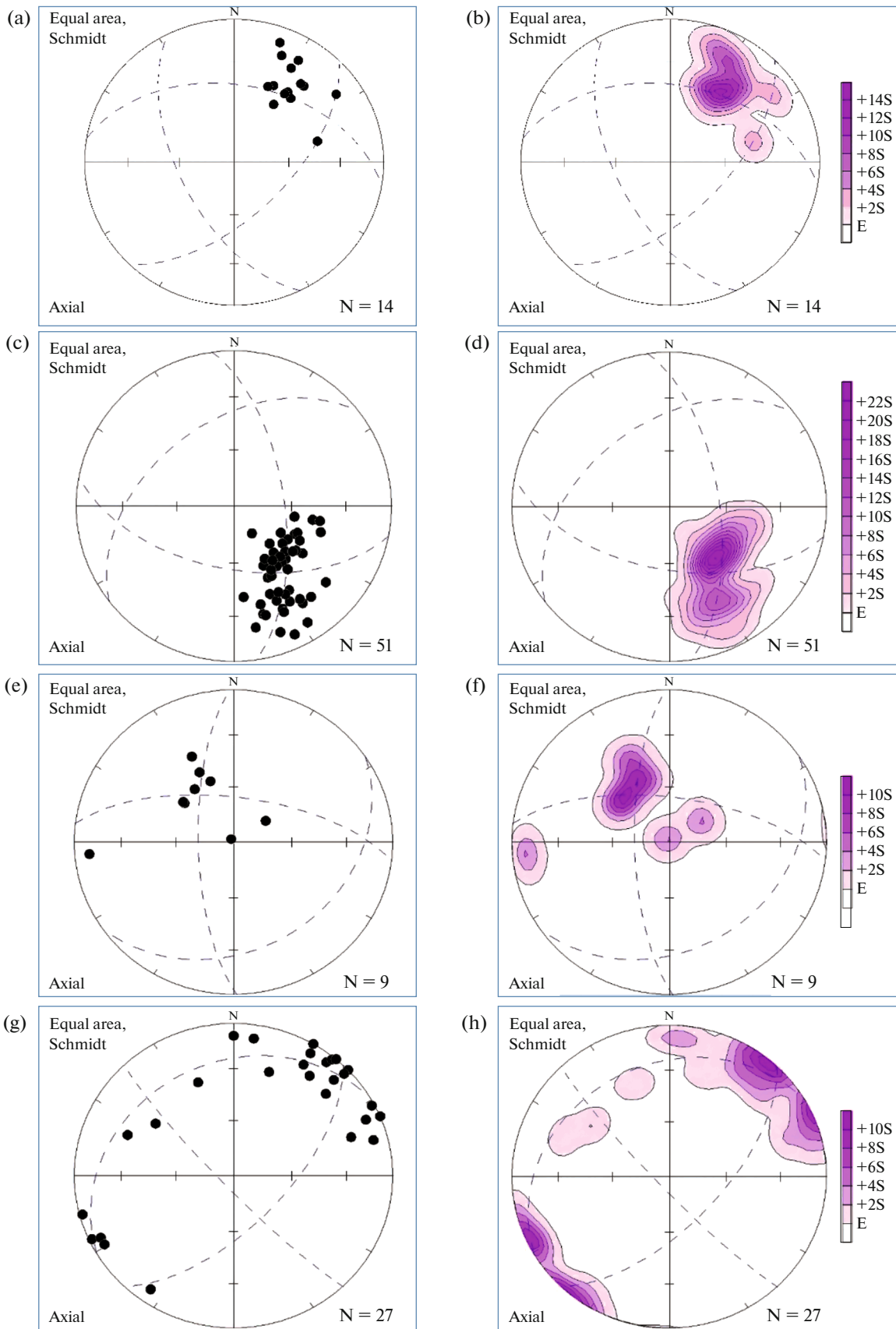
D_3 Deformation Phase

The structures produced by the D_3 deformation comprise pervasive vertical to inclined mesoscopic open to very open folds (F_3), with axes plunge NW (to NNW) and SE (to SSE) at moderate to steep angles. F_3 is defined regionally by a systematic change of dip direction of pre-existing $S_2//S_1$ fabrics, as well as the development of S_3 strain slip cleavage and axial plane foliation. S_3 planar fabric strike NW (to NNW)–SE (to SSE) with NE (to ENE) and SW (to WSW) steep dipping. F_3 is frequently accompanied by a rigorous L_3 crenulation or spaced cleavage; L_3 is frequently coaxial to the F_3 folding axes. Overprinting of F_3 folds on older F_2 or F_1 folds locally produces a complex interference pattern. At map-scale and also at some outcrops, the effect of F_3 folding is remarkably weakly developed and discontinuous and as such do not considerably affect the major and minor F_2 thrust-related folds and earlier formed structures outcropping in the mapped area. The formation of the D_3 structures is considered to have taken place during an ENE-WSW shortening phase affected the study area and probably the entire south Eastern Desert tectonic in northwestern Arabian-Nubian Shield.

Fig. 5. Stereoplots of the collected data from Domain I. (a) Pole diagram and (b) its contour equivalents for orientational data (lower hemisphere equal area projection) of the poles to F_2 small fold hinges and L_2 lineation (11 readings). (c) Pole diagram and (d) its contour equivalents for orientational data (lower hemisphere equal area projection) of the poles to S_2 foliation (70 readings). (e) Pole diagram and (f) its contour equivalents for orientational data (lower hemisphere equal area projection) of the poles to F_3 small fold hinges and L_3 lineation (6 readings). (g) Pole diagram and (h) its contour equivalents for orientational data (lower hemisphere equal area projection) of the poles to S_3 foliations (15 readings). Contours per unit area are observed to the right of the diagram.

D_4 Deformation Phase

The latest D_4 deformation phase in the concerned area is represented by abundant small- and large-scales WNW–ESE trending semi-ductile semi-brittle shear zones. The obvious Wadi Kharit Shear Zone is affiliated to this phase of deformation based on the fact that transcurrent shearing overprinted the earlier formed structures. Shearing along Wadi Kharit, in the framework of the study area, was evidently dextral as indicated by kinematic indicators with monoclinic symmetry encountered at outcrop-scale and detected under the microscope. Such dextral shearing led to the formation of well-developed F_4 shear zone–related folding and passive-roofed thrust duplexing. Parallel to Wadi Kharit Shear Zone there are dykes, and quartz and pegmatite veins that are themselves traversing and crosscutting the F_2 map-scale thrust-related folds and the accompanied mesoscopic overturned folds. L_4 lineation is mainly stretching lineation confirming the vector of greatest stretching parallel to the main Wadi Kharit shearing and perpendicular to the principle plane of shortening. Stretching lineation is encountered along the pre-existing S_2 foliation as a nearly subhorizontal fabric element. Detailed structural map of the whole study area shown in Fig. 9.
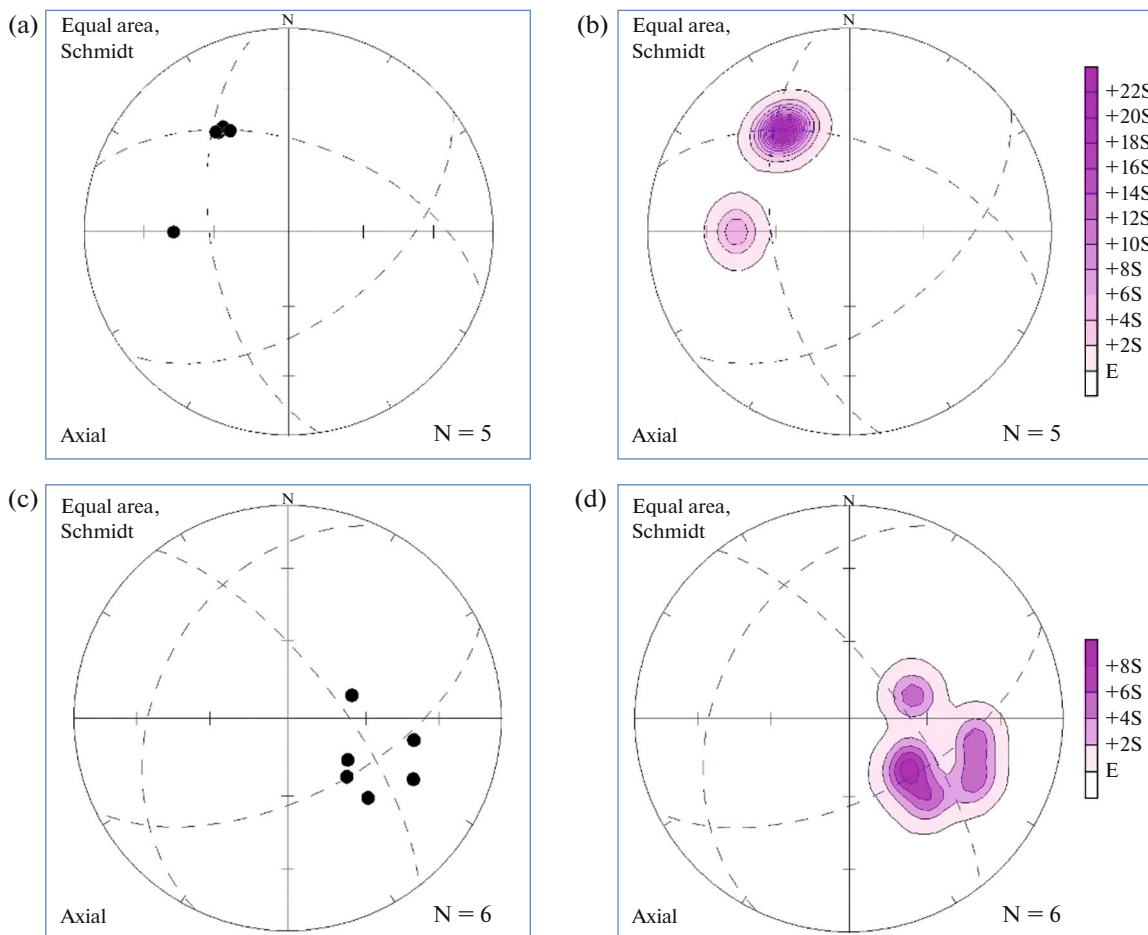
Fig. 7. Stereoplots of the collected data from Domain III. (a) Pole diagram and (b) its contour equivalents for orientational data (lower hemisphere equal area projection) of the poles to F_2 small fold hinges and L_2 lineation (5 readings). (c) Pole diagram and (d) its contour equivalents for orientational data (lower hemisphere equal area projection) of the poles to S_2 foliations (6 readings). Contours per unit area are observed to the right of the diagram.
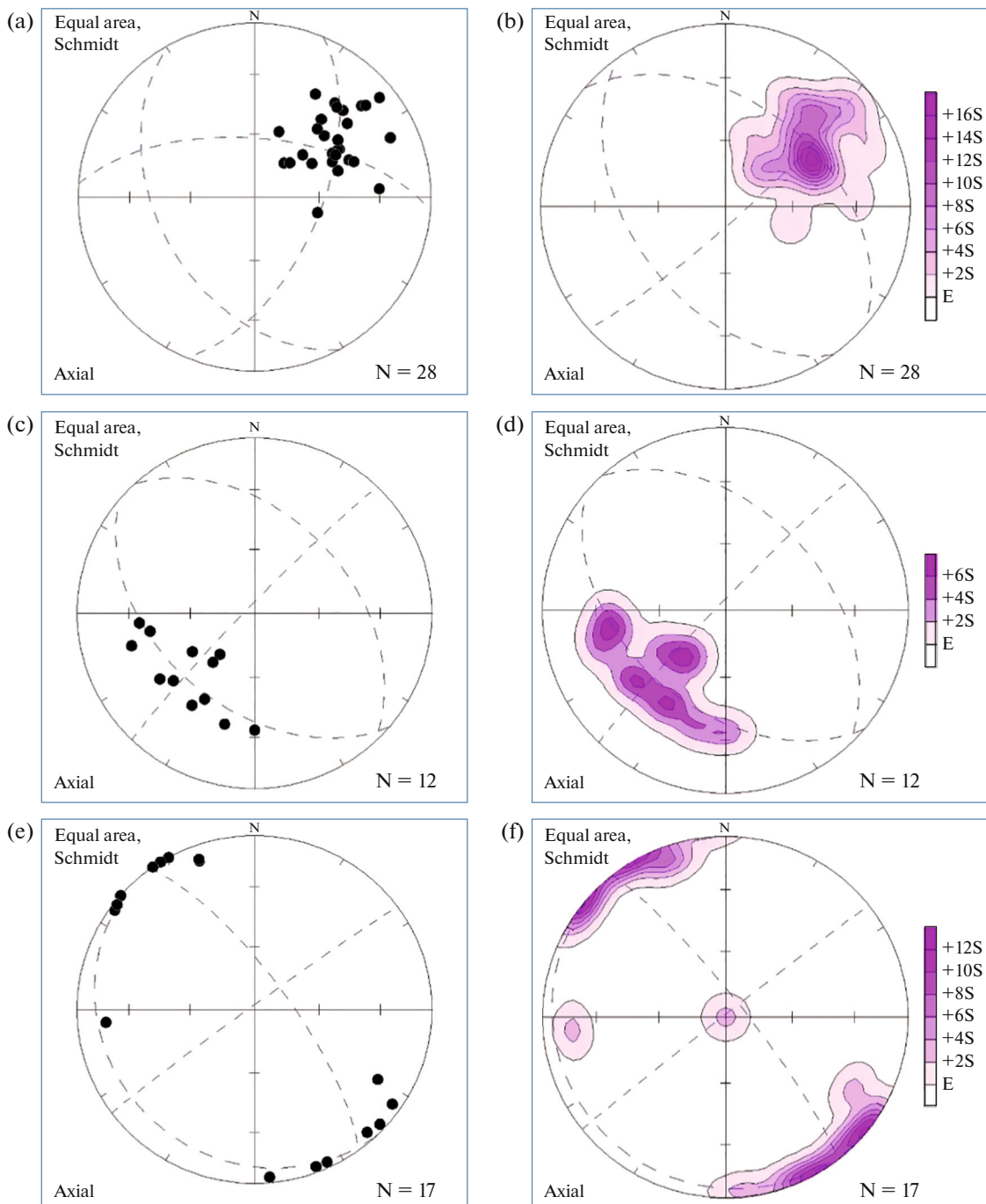
Fig. 8. Stereoplots of the collected data from Domain IV. (a) Pole diagram and (b) its contour equivalents for orientational data (lower hemisphere equal area projection) of the poles to F_2 small fold hinges and L_2 lineation (28 readings). (c) Pole diagram and (d) its contour equivalents for orientational data (lower hemisphere equal area projection) of the poles to S_2 foliation (12 readings). (e) Pole diagram and (f) its contour equivalents for orientational data (lower hemisphere equal area projection) of the poles to S_3 foliation (17 readings). Contours per unit area are observed to the right of the diagram.

TECTONIC FRAMEWORK

Juxtaposition of the Eastern Desert Terrane to the Gabgaba Terrane was the consequence of a NNE−SSW contractional phase (~750−660) (Fig. 10a). This phase resulted in the formation of structural fabrics referring in the present study as D_1 structures (tight to very tight F_1 isoclinal folds, tightly appressed fold closures and sheared-out hinges, and associated S_1 axial plane foliation, as well as L_1 mineral and stretching lineations). A subsequent NW (to NNW)−SE (to SSE) contraction was responsible for the formation of D_2 structures. These structures include minor- and
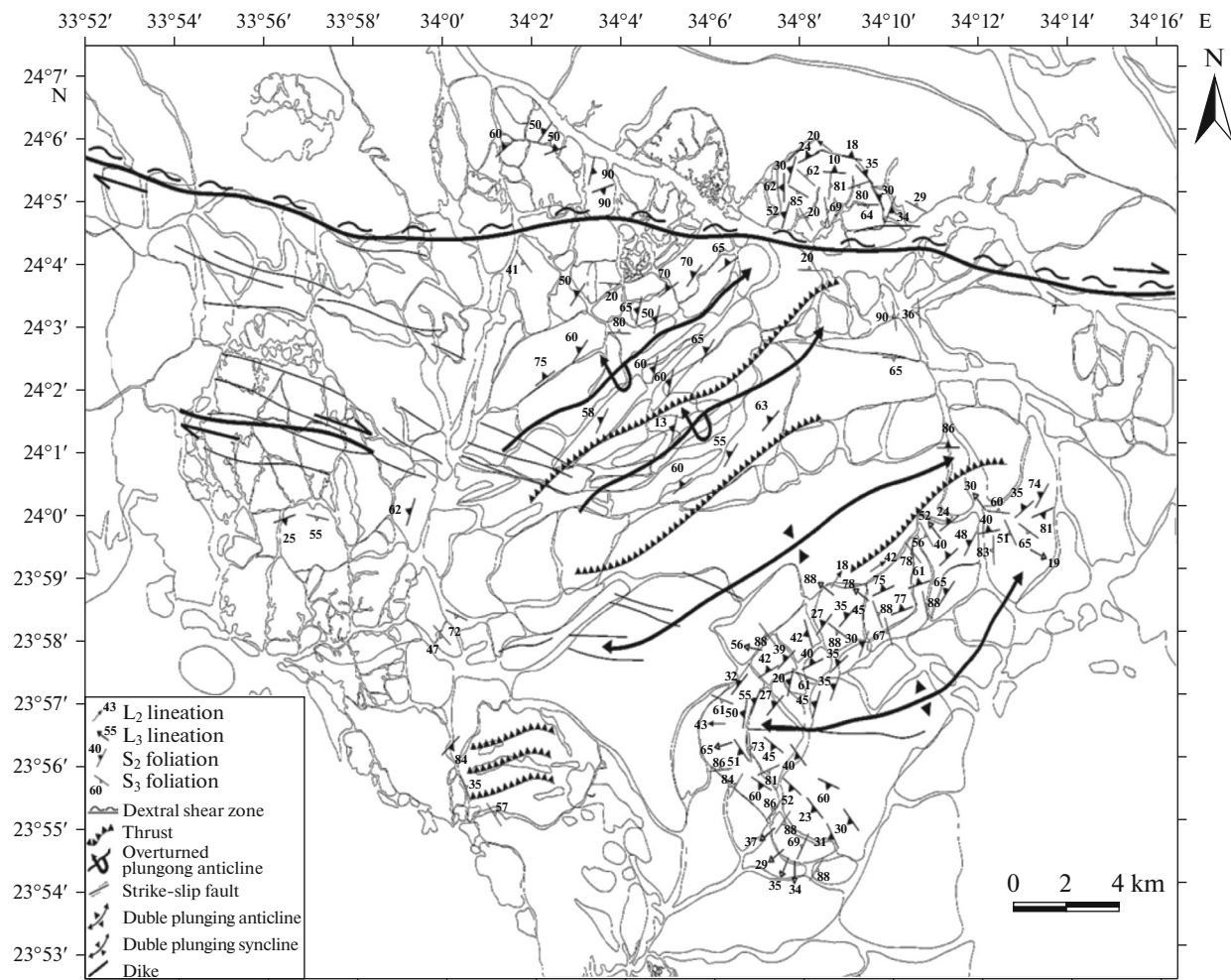
**Fig. 9.** Detailed structural map of Urf Al-Mahib area.

map-scale prominent F_2 overturned folds with axial planes striking NE (to ENE)−SW (to WSW) and dipping NW (to NNW) by moderate angles. F_2 folds are geometrically- and kinematically-related to thrust propagation, and often have SE (to SSE) vergency (Fig. 10b, c). A third attenuated NE (to ENE)−SE (WSW) contract gave the D_3 structures that contain pervasive vertical to inclined mesoscopic open to very open folds (F_3), with axes plunge NW (to NNW) and SE (to SSE) at moderate to steep angles. The Late Neoproterozoic Hamisana Shear Zone shown in Fig. 10a is most probably affiliated to a post-D_3 deformation phase. This zone represents a part of a major escape (indentation) tectonic zone extending to the north of Gerf Nappe which is itself the largest ophiolitic nappe all over the ANS and at the same time regarded as one of several lines of evidence for escaping towards the north. The Hamisana Shear Zone juxtaposed Gabgaba versus Gebeit Terranes. The structural architecture of the study area and the whole district around Wadi Kharit was completed by the

youngest Late Neoproterozoic D_4 deformation phase which is manifested by abundant small- and large-scales WNW−ESE trending semi-ductile semi-brittle shear zones. The obvious Wadi Kharit Shear Zone is affiliated to this phase of deformation based on the fact that transcurrent shearing overprinted the earlier formed structures. Several lines of evidence (such as: veins, deflected markers, S−C structures, microscale foliations, porphyroclasts, mica fish and mineral fish) reflect a dextral-sense of shearing along the main Wadi Kharit Shear zone, at least within the frame of the present study area. Such dextral shearing resulted in creations of well-developed F_4 shear zone−related folding and passive-roofed thrust duplexing.

CONCLUSIONS

The main conclusions of the present work are the following.

(1) The exposed lithologies in the area are discriminated into: metasediments, metagabbro-diorite
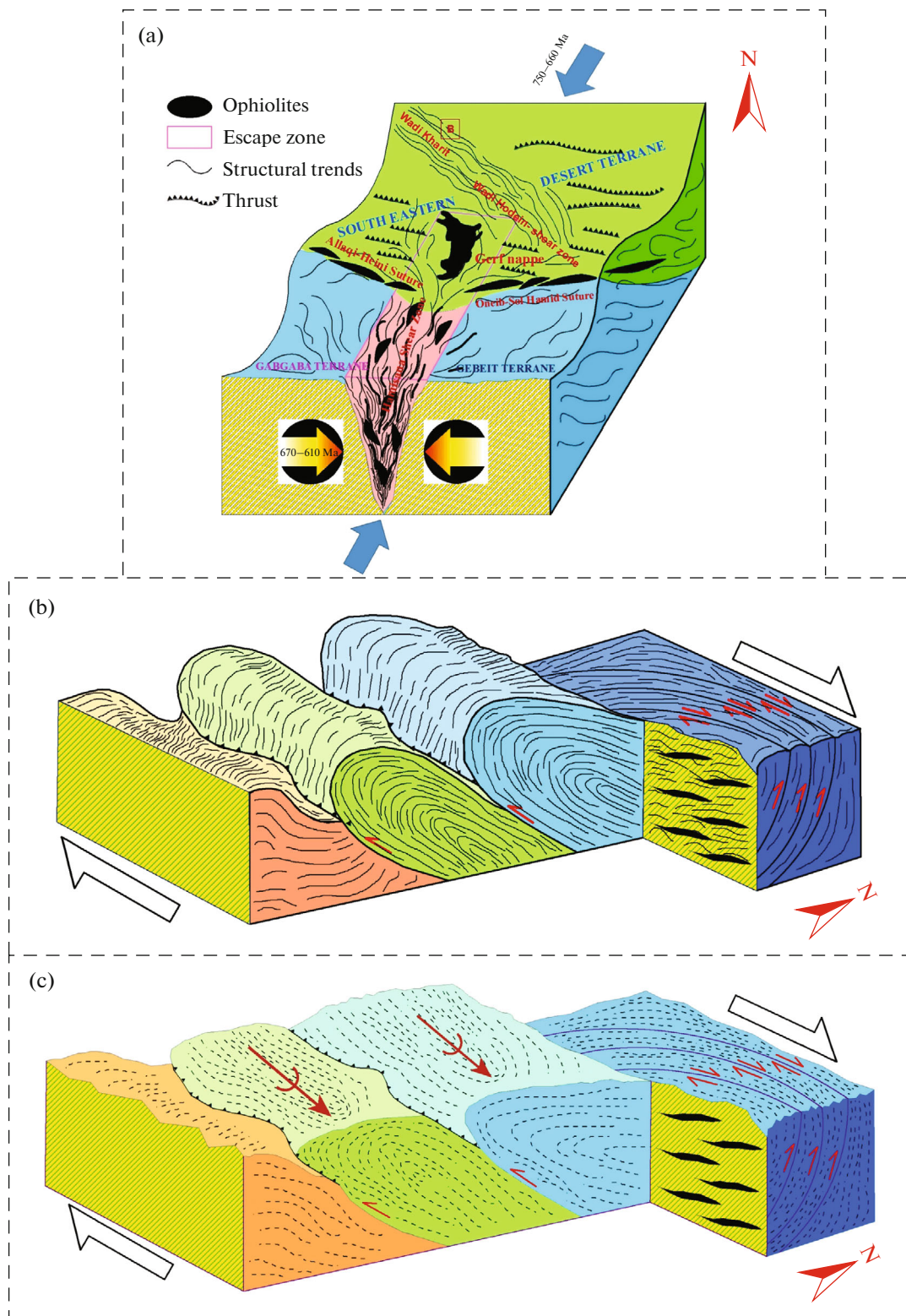
Fig. 10. Three-dimensional cartoon illustrating a preferred sequence of tectonic events in Urf Al-Mahib area, Eastern Nubian Shield, Egypt. 3-D cartoons illustrating the tectonic evolution of Urf Al-Mahib area (Wadi Kharit District) within the frame of the regional setting of south Eastern Desert, Gabgaba and Gebeit tectonic terranes. (a) Juxtaposition of the south Eastern Desert (Gerf or Aswan) in one hand and Gabgaba-Gebeit terranes on the other hand along the Allaqi-Heini-Oneib-Sol Hamid Suture. The Gabgaba and Gebeit terranes are separated along the Hamisana Shear Zone which is regarded by many workers as escape tectonic zone (indentation zone). (b, c) Simplified block diagram exhibiting the main structural fabrics and tectonic evolution of the study area. Notice, dextral-sense of shearing along Wadi Kharit and the positive flower structure recorded within the vicinity of the main shear zone.

complex, syn-to late-tectonic granitoids, post-tectonic granites, post-granitic dykes and Phanerozoic sediments.

(2) Structural succession in the area involves four phases of deformation (D_1, D_2, D_3 and D_4).

(3) D_1 phase was concurrent with the suturing between Eastern Desert Terrane and Gabgaba Terrane. D_1-related structures are strongly affected by the latter deformations.

(4) D_2 was an intensive phase resulted in the formation of minor- and map-scale prominent F_2 overturned folds with NW (to NNW)-dipping long upper limbs and short lower overturned limbs and axial planes striking NE (to ENE)−SW (to WSW).

(5) D_3 is represented in the study area by pervasive vertical to inclined mesoscopic open to very open folds (F_3), with axes plunge NW (to NNW) and SE (to SSE) at moderate to steep angles.

(6) The conspicuous Wadi Kharit Shear Zone belongs to the D_4 phase. Several lines of evidence prove dextral sense of movement along Wadi Kharit Shear Zone.

(7) It could be regarded as a conclusive evidence that either Wadi Kharit Shear Zone is not representing the northwestern continuation of the Wadi Hodain left-lateral Transcurrent High Strain Zone, or (in case of the presence of a mutual relation between both megshears) the recorded dextral shearing in Urf Al-Mahib area may indicate that the Najd-related Wadi Hodain−Wadi Kharit megashear was overprinted by dextral shearing subsequent to the main sinistral shearing. The latter interpretation should be taken into consideration during the investigation of the Najd-related corridor in the Eastern Desert (Aswan or Gerf) Tectonic Terrane and in the entire ANS.

REFERENCES

1. S. El-Gaby, F. K. List, and R. Tehrani, "The basement complex of the Eastern Desert and Sinai," in *The Geology of Egypt*, Ed. by R. Said (Balkema, Rotterdam, 1990), pp. 175−184.

2. W. Frisch, and A. Al-Shanti, "Ophiolite belts and the collision of island arcs in the Arabian Shield," Tectonophysics **43**, 293−306 (1977).

3. Z. Hamimi, M. A. Abd El-Wahed, H. A. Gahlan, and S. Z. Kamh, "Tectonics of the Eastern Desert of Egypt: Key to understanding the Neoproterozoic evolution of the Arabian-Nubian Shield (East African Orogen)," in *The Geology of the Arab World − An Overview* (Springer, 2019), pp. 1−81.

4. Z. Hamimi, M. El-Shafei, G. Kattu, and M. Matsah, "Transpressional regime in southern Arabian Shield: Insights from Wadi Yiba Area, Saudi Arabia," Mineral. Petrol. **107**, 849−860 (2013).

5. A. M. Hopgood, *Determination of Structural Successions in Migmatites and Gneisses* (Kluwer, Dordrecht, 1999).

6. P. R. Johnson, and B. Woldehaimanot, "Development of the Arabian-Nubian Shield: Perspectives on accretion and deformation in the northern East African Orogen and the assembly of Gondwana," in *Proterozoic East Gondwana: Supercontinent Assembly and Breakup*, Vol. 206 of *Geol. Soc. London, Spec. Publ.*, Ed. by M. Yoshida, B. E. Windley, and S. Dasgupta (London, 2003), pp. 289−325.

7. A. Kröner, "Ophiolites and the evolution of tectonic boundaries in the late Proterozoic Arabian—Nubian shield of northeast Africa and Arabia," Precambrian Res. **27**, 277−300 (1985).

8. A. Kröner, and R. J. Stern, "Pan-African Orogeny," in *Encyclopedia of Geology*, Vol. 1 (N.Y., Elsevier, 2005).

9. P. H. Kuenen, "Graded bedding with observations on Lower Paleozoic rocks of Britain," K. Ned. Akad. Wet. Afd. Nat. Verh., 1st Ser. **20** (3), 1−47 (1953).

10. A. C. Ries, R. M. Shackleton, R. H. Graham, and W. R. Fitches, "Pan-African structures, ophiolites and mélange in the Eastern Desert of Egypt: A traverse at 26 N," J. Geol. Soc. (London, U. K.) **140**, 75−95 (1983).

11. R. J. Stern, "Arc-assembly and continental collision in the Neoproterozoic African orogen: Implications for the consolidation of Gondwanaland," Annu. Rev. Earth Planet. Sci. **22**, 319−351 (1994).

12. R. J. Stern, "Crustal evolution in the East African Orogen: a neodymium isotopic perspective," J. Afr. Earth Sci. **34** (3), 109−117 (2002).

13. R. J. Stern, P. R. Johnson, A. Kröner, and B. Yibas, "Neoproterozoic ophiolites of the Arabian-Nubian shield," in *Precambrian Ophiolites and Related Rocks*, Vol. 13 of *Dev. Precambrian Geol.*, Ed. by T. M. Kusky (Elsevier, 2004), pp. 95−128.

14. E. Ten Haaf, "Significance of convolute lamination," Geol. Mijnbouw **18**, 188−194 (1956).

15. Geotechpedia, Spheristat 3.2.1. http://geotechpedia.com/Software/Show/510/SpheriStat. Accessed May 25, 2015.